

State-Selected Ion-Molecule Reactions Studied by the Threshold Electron-Secondary Ion Coincidence (TESICO) Technique, $Ar^+(^2P_{3/2}, ^2P_{1/2}) + HCl$

Takahiro Fukuzumi, Ryousuke Nakano, Satoshi Okamura, Kenji Honma,* and Inosuke Koyano

Department of Material Science, Himeji Institute of Technology, Kamigori, Hyogo 678-1297

(Received July 19, 2001)

The reactions of Ar^+ with HCl were studied for the two spin-orbit states of Ar^+, $^2P_{3/2}$ and $^2P_{1/2}$, by the threshold electron-secondary ion coincidence (TESICO) technique. State selected relative reaction cross sections of the two product channels, hydrogen abstraction (HA) to form ArH^+, and charge transfer (CT) to form HCl^+, were determined at five collision energies in the range of 0.71–3.5 eV. At low collision energies, the cross sections of both channels show no substantial difference between the two spin-orbit states. At high collision energies, the cross sections for the HA channel also show no difference between the two states, whereas those for the CT channel show significant dependence on the spin-orbit state, the cross sections for $Ar^+(^2P_{1/2})$ being always larger than those for $Ar^+(^2P_{3/2})$. Combining these results with the coincidence time-of-flight (TOF) spectra, a direct reaction mechanism is suggested for both channels. The importance of the nonadiabatic transitions between the surfaces correlating to the $Ar^+ + HCl$ and $Ar + HCl^+(A^2\Sigma)$ states in leading the reaction is proposed. Proton transfer follows the nonadiabatic transition for the HA channel and radiative or nonradiative transition follows for the CT channel.

One characteristic property of ion-molecule reactions, $AB^+ + CD$, is that more than two potential energy surfaces participate in the reaction and nonadiabatic transitions between them play an important role. The potential surface evolving from the charge transferred product, $AB + CD^+$, usually lies closely in energy to the reactant surface and vibronically mediated near resonance between the two surfaces plays a key role in the outcome of the whole reactions.[1,2] In the reaction of $Ar^+ + H_2$ (D_2), cross sections have been measured for the two spin-orbit states of the reactant ion, $Ar^+(^2P_{3/2}, ^2P_{1/2})$, and enhancement of the cross sections for $Ar^+(^2P_{1/2})$ has been observed for two product channels, hydrogen abstraction (HA) to form ArH^+ and charge transfer (CT) to form H_2^+. These results have been interpreted by the nonadiabatic transitions occurring at long intermolecular distances between the reactant surface and the surface evolving from $Ar + H_2^+$, the latter adiabatically leading to both products, $Ar + H_2^+$ and $ArH^+ + H$. This nonadiabatic transition is suggested as vibrationally mediated and the near resonance between $Ar^+(^2P_{1/2}) + H_2$ and $Ar + H_2^+$ ($v = 2$) as responsible for the enhancement of the cross sections of $Ar^+(^2P_{1/2})$.[1]

When more than three potential surfaces participate, the situation becomes more complicated. The reaction systems $(Ar + CD)^+$, where CD is O_2 or NO, represent examples of such cases. In these systems, multi-surface interaction must be taken into consideration for the forward reaction (starting from $Ar^+ + CD$) because the third surface originating from the $Ar + CD^{+*}$ state lies between the two product surfaces[3] and hence heavily participates in the reaction. In fact, the energy dependence of the state selected charge transfer cross sections for the $Ar^+ + CD$ reaction could not be interpreted by the simple two-state model using the energy defects and Franck–Condon factors, whereas that of the state selected charge transfer cross sections for the $Ar + CD^{+*}$ reaction could be interpreted reasonably well in terms of these molecular properties.[2,4] Unfortunately these systems only have the CT channel and it is not yet clear how a rearrangement reaction channel is affected by the multi-surface interaction.

In the present paper, we present an experimental study of the reaction of Ar^+ with HCl. This reaction has been studied by ICR (Ion Cyclotron Resonance)[5] and SIFDT (Selected Ion Flow Drift Tube)[6,7] techniques at near thermal to a few eV collision energy and by ion beam-gas cell technique at higher collision energies.[8] Although there exist some small discrepancies in the branching ratios among these studies, product channels have been confirmed as charge transfer (CT) [reaction (1a)] and hydrogen abstraction (HA) [reaction (1b)].

$$Ar^+(^2P_{3/2}, ^2P_{1/2}) + HCl \rightarrow Ar + HCl^+(X^2\Pi_{3/2,1/2}) \quad (1a)$$
$$\rightarrow ArH^+ + Cl \quad (1b)$$

From the state correlation viewpoint, this system is analogous to the $Ar^+ + H_2$ (D_2) system, but more complicated by the involvement of multiple potential surfaces. That is, neither the ground state of the HA product, ArH^+, nor the CT product, $HCl^+(X^2\Pi_{3/2,1/2})$, correlates to the ground state of the reactant adiabatically as shown in Fig. 1. ArH^+ and $HCl^+(X^2\Pi_{3/2,1/2})$ correlate only to $Ar + H^+$ (not to $Ar^+ + H$)[9] and $H + Cl^+$, respectively. Because the electronically excited $HCl^+(A^2\Sigma)$ lying 0.47 eV above the reactant state correlates to $H^+ + Cl$, nonadiabatic transition from the surface of $Ar^+ + HCl(X)$ to that of $Ar + HCl^+(A^2\Sigma)$ is expected to play a key role in this

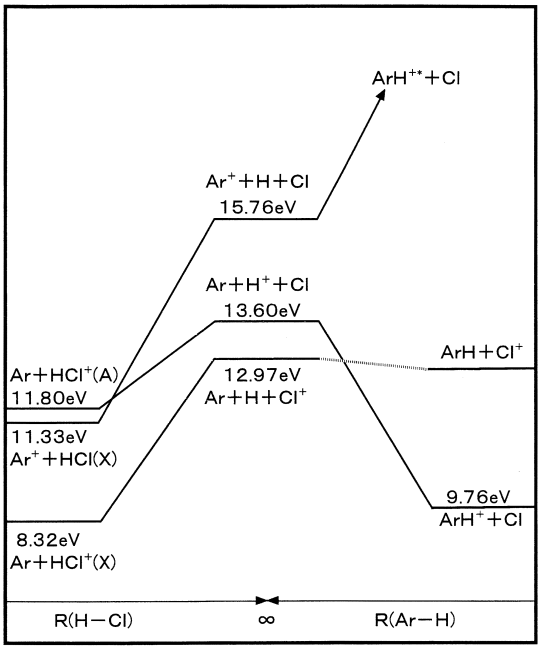

Fig. 1. Correlation diagram for several reactant and product states relevant to the system studied here. For Ar^+ + HCl, the energy of $Ar^+(^2P_{3/2})$ + HCl is shown. All energies are given with respect to Ar + H + Cl and obtained from K. P. Huber and G. Herzberg, "Molecular Spectra and Molecular Structure IV Constants of Diatomic Molecules," Van Nostrand Reinhold Company (1979), and S. G. Lias, J. E. Bartmess, J. F. Liebman, J. L. Holmes, R. D. Levin, and W. G. Mallard, *J. Phys. Chem. Ref. Data*, **17**, Suppl. 1 (1988).

reaction. Experimentally the formation of $HCl^+(A^2\Sigma)$, reaction (1c), has been suggested by the SIFDT experiment.[6]

$$Ar^+(^2P_{3/2}, ^2P_{1/2}) + HCl \rightarrow Ar + HCl^+(A^2\Sigma) \qquad (1c)$$

The kinetic energy dependence of the rate constant of reaction (1) shows a minimum, which was explained by the occurrence of two mechanisms, direct and indirect ones. The former, which is responsible for the reaction at higher kinetic energies, was suggested to have an energy threshold corresponding to the formation of $HCl^+(A^2\Sigma)$. The formation of $HCl^+(A^2\Sigma v = 0–6)$ has been directly observed by the ion beam chemiluminescence technique, however, the formation of a long-lived complex was insisted for reaction (1c) because the cross section decreases with the collision energy up to 10 eV.[8]

In the present study, relative reaction cross sections of reactions (1a) and (1b) were determined for the two spin-orbit states of $Ar^+(^2P_{3/2}, ^2P_{1/2})$ by the threshold electron-secondary ion coincidence (TESICO) technique at five collision energies in the range of 0.71–3.5 eV. The results were compared with a simple model based on the energy defects and Franck–Condon factors. This model is expected to represent the cross sections of reactions controlled by long-range nonadiabatic transitions reasonably well.[2] The coincidence time-of-flight (TOF) data were also analyzed to obtain useful information about the reaction mechanism.

Experimental

The threshold electron-secondary ion coincidence (TESICO) technique and the apparatus have been described in detail elsewhere.[10] Briefly, the apparatus consists of a helium Hopfield continuum light source, a 1 m Seya–Namioka monochromator, an ionization chamber, a reaction chamber, a steradiancy threshold electron analyzer, and a quadrupole mass spectrometer, these being assembled together via a six-stage differential pumping system. The reactant Ar^+ ions are produced by photoionization of Ar at the threshold wavelength for each spin-orbit state. The ions produced in the ionization chamber are extracted, formed into a beam of desired velocity, and injected into the reaction chamber filled with the neutral reagent HCl. The pressure in the reaction chamber was kept low enough to suppress secondary collisions. The product ions produced there, as well as unreacted primary ions, are extracted from the chamber, mass analyzed, and detected in coincidence with the threshold electron signals obtained on the opposite side of the ionization chamber. Coincidence measurements are performed by feeding the threshold photoelectron and mass-analyzed ion signals into the start and stop input, respectively, of a time-to-pulse height converter and analyzing the resulting output signals by a multichannel pulse height analyzer. The raw data obtained are thus the coincidence TOF spectra for the primary and secondary ions. From the ratios of the integrated intensities of these primary and secondary ion peaks, the relative reaction cross sections for individual states are obtained directly. The collision energy was determined by the difference between the voltages applied to the ionization and reaction chambers, and the width was estimated to be ± 0.3 eV.

High purity sample gases, Ar (Taiyo sanso) and HCl (Sumitomo seika), were used without further purification. Their nominal purities are higher than 99.999% for Ar and 100 v/v% for HCl.

Results and Discussion

Coincidence Spectra of the Primary and Secondary Ions with Threshold Electrons. Two ions, ArH^+ and HCl^+, were observed as secondary ions at all collision energies studied and weak signals of Cl^+ were also observed at collision energies higher than 1.0 eV. Two major products are consistent with the previous studies by ICR[5] and SIFDT[6,7]. The Cl^+ ion is likely a product of dissociative charge-transfer and may not be formed under low collision energies used in the ICR and SIFDT studies. The H^+ and $ArCl^+$ ions could not be measured because their mass numbers are not accessible by our quadrupole mass filter.

A typical example of the coincidence TOF spectra of the primary Ar^+ and secondary ions with threshold electrons is shown in Fig. 2. Because the spectra were taken at 77.75 nm (threshold wavelength for the $Ar^+(^2P_{1/2})$ excited state), the detected ions correspond to $Ar^+(^2P_{1/2})$ and the secondary ions produced from this reactant. The coincidence TOF spectra measured at 78.65 nm (threshold wavelength for the $Ar^+(^2P_{3/2})$ ground state) and those at the other collision energies are qualitatively identical to the spectra shown in Fig. 2. In principle, the relative reaction cross sections can be determined from the ratios of the integrated intensities of the coincidence peaks for the primary and secondary ions. However, the presence of $^{36}Ar^+$, accounting for 0.34% of $^{40}Ar^+$, must be taken into account in analysing the coincidence spectrum of HCl^+. Based

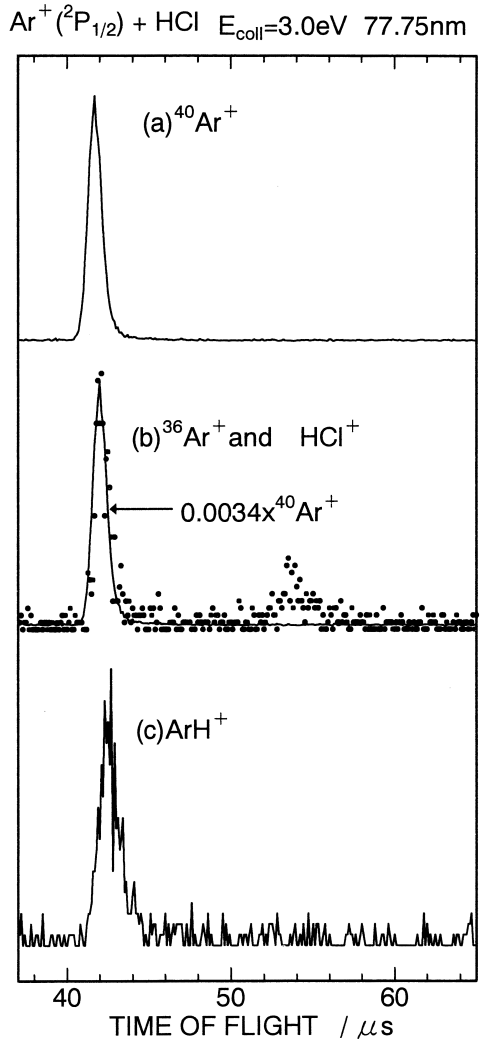

Fig. 2. Coincidence time-of-flight (TOF) spectra measured at 77.75 nm, which is the threshold wavelength to form $Ar^+(^2P_{1/2})$. They are measured at 3.0 eV of collision energy for (a) $^{40}Ar^+$, (b) $^{36}Ar^+$ and HCl^+, and (c) ArH^+.

on the reasonable assumption that unreacted $^{36}Ar^+$ has an identical TOF profile to that of $^{40}Ar^+$, the contribution of $^{36}Ar^+$ shown in Fig. 2(b) by the solid line was subtracted from the coincidence spectrum for the secondary ions having $m/z = 36$ as shown. The small difference in the flight times between $^{36}Ar^+$ and $^{40}Ar^+$ has been taken into account. It is clear from Fig. 2(b) that the sharp peak at the shorter TOF (42 μs) entirely originates from unreacted $^{36}Ar^+$ and the real CT product, HCl^+, shows up as the small peak at the longer TOF (54 μs). After the subtraction, the relative reaction cross sections were determined for the two product channels and are summarized in Fig. 3.

It has been shown that the coincidence TOF spectra as given here provide insight into the reaction mechanism.[11] The TOFs of ions are determined by the velocities of the ions at the exit of the reaction chamber and by the distance between that place and the detector. In the beam-chamber method, the primary ions (Ar^+) entering the reaction chamber have been accelerated to a velocity larger than the one corresponding to the thermal energy at ambient temperature, whereas the neutral molecules in the reaction chamber are in thermal motion. Thus, the product ions formed by light-atom abstraction, typically H atom abstraction, have almost the same velocity as the primary ion, while those formed by charge-transfer without momentum transfer have slower velocities because they can not have any initial velocity other than the thermal motion. The ions formed by an intermediate complex mechanism probably have velocities in between these two because they are expected to have symmetric velocity distribution with respect to the center-of-mass of the reaction system.

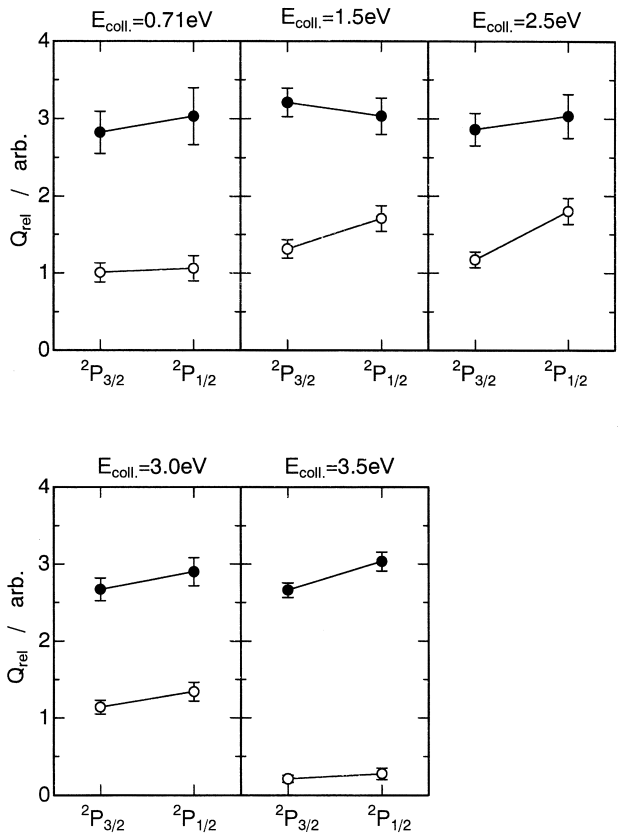

Fig. 3. Relative reaction cross sections for the HA (●) and CT (○) channels. The error bars are given by $\pm 1\sigma$ of the measurement.

From the above viewpoint, the coincidence TOF spectra shown in Fig. 2 provide some important information about the mechanism. At first, the ArH^+ ion is suggested to have been formed by a direct hydrogen atom abstraction rather than via a complex mechanism, since its TOF is almost identical to that of the primary ion. Although ArH^+ appears at slightly longer TOF than Ar^+, the difference is attributed to the difference in m/z. It must be noted that this result does not rule out a mechanism such as the direct CT (forming $Ar + HCl^+$) followed by the proton-transfer (forming $ArH^+ + Cl$). In this sequential mechanism, the original velocity of Ar^+ is kept in the final product ArH^+. Compared with ArH^+, the HCl^+ ion shows longer TOF in spite of its smaller m/z. This result is reasonable because neither of the two possible mechanisms to form HCl^+, the complex mechanism or the direct CT, can form product ions with a high velocity comparable to that of the primary ion.

Because the electric field applied to the reaction chamber makes it difficult to estimate the TOF for the center-of-mass of the reaction system, the coincidence TOF spectrum alone can not determine which mechanism is responsible for or dominates in the formation of HCl^+.

Relative Reaction Cross Sections. From Fig. 3, it can be seen that, for all collision energies studied, HA (reaction (1b)) has larger cross sections than CT (reaction (1a)) for both of the two spin-orbit states. Branching ratios of HA and CT have been determined by SIFDT studies. Glosik et al. reported that the CT channel is dominant and the HA channel contributes only 10–20% of the CT channel in the collision energy range of 0.04–3.0 eV.[6] This is contrary to the relative importance of the two channels observed in the present study. This discrepancy could be explained by the difference in the collecting efficiencies of ions formed by different mechanisms. As discussed in the previous section, the product ions of the two channels, ArH^+ and HCl^+, have different velocities in the reaction chamber. It is reasonable that the ArH^+ ion having higher velocity along the detection axis is favorable to be detected far more than HCl^+.

Relative cross sections for the two spin-orbit states show a common trend over the collision energies studied. For the HA channel, the cross sections for the two states are identical within the experimental error. On the other hand, those for the CT channel show a small discrepancy except for the case of 0.71 eV of collision energy; the cross sections for $Ar^+(^2P_{1/2})$ is always larger than those for $Ar^+(^2P_{3/2})$. These trends are more clearly seen by plotting the ratios of cross sections for the two spin-orbit states, as shown in Fig. 4. The ratios for the HA channel are seen to be unity at all collision energies (Fig. 4 (b)), while those for the CT channel are larger than unity (Fig. 4(a)).

Model Calculation. As mentioned in the Introduction, a nonadiabatic transition from the reactant surface, $Ar^+ + HCl$, to the charge-transferred surface, $Ar + HCl^+(A^2\Sigma)$, is necessary in order for both products to be formed. Such nonadiabatic transitions have been classified into two types, direct and intimate ones, or Demkov type and Landau–Zener type.[2] Kato has shown that the relative reaction cross sections for the charge transfer reaction via direct mechanism can be well reproduced by the energy defects and Franck–Condon factors between the two states involved, while those for the reaction via intimate collision mechanism can not be given by these molecular properties at infinite separation. In the present study, we also calculated the ratios of the cross sections for the two spin-orbit states for the two product channels, HA and CT, by the simple model based on the energy defects and Franck–Condon factors, as shown in Fig. 4. The details of the calculation are described elsewhere.[4] The model is based on the assumption that each product state can be treated independently as a two-state problem to which the impact parameter theory of Rapp and Francis[12] can be applied. The cross sections for each specific pair of the reactant and product states of $Ar^+(^2P_j) + HCl\ (v = 0) \rightarrow Ar + HCl^+(v')$ are first calculated according to the Rapp and Francis formula. The charge transfer cross sections for each selected initial state are then obtained by summing up the contributions from each product state multiplied by the weight of the Franck–Condon (FC) factor. The summation is taken over $v = 0$ to 6 of $HCl^+(A^2\Sigma)$ because vibrational states of $v \geqq 7$ are predissociated to $H(^2S) + Cl^+(^3P)$.[13] The FC factors for the $HCl \rightarrow HCl^+(A^2\Sigma)$ transition given by Hotop et al. were used.[14] Although some low vibrational levels of $HCl^+(X^2\Pi)$ having large FC factors were also taken into account,[15] their contribution were more than two orders of magnitude smaller than those of $HCl^+(A^2\Sigma)$ because of the large energy defects.

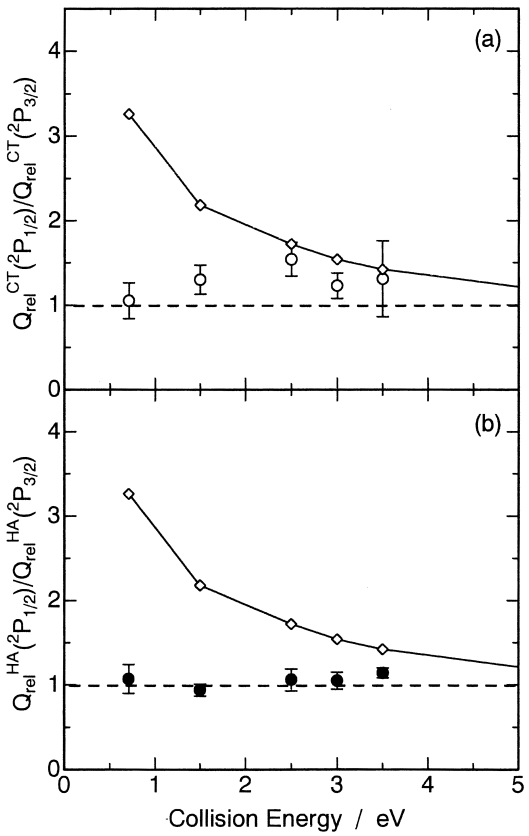

Fig. 4. Ratios of the cross sections for the two spin-orbit states plotted as a function of the collision energy; (a) the charge-transfer channel, (b) the hydrogen atom abstraction channel. Solid lines and diamonds (◇) are the ratios calculated by the model described in the text.

The calculated ratios are shown in Fig. 4 by diamond (◇) connected with solid lines. They decrease monotonically with increasing collision energy and become almost unity at 6–7 eV. The observed ratios for the HA channel do not agree with the calculated ones at all collision energies (Fig. 4(b)). The ratios for the CT channel are also much smaller than the calculated ones at low collision energies, but they show reasonable agreement at higher (say, > 2.5 eV) collision energies (Fig. 4(a)).[16]

Proposed Reaction Mechanism. These results suggest that the transition between the $Ar^+ + HCl$ and $Ar + HCl^+(A^2\Sigma)$ surfaces at large reactants' separation, i.e. Demkov type transition, is not efficient at low collision energies. In the Demkov type mechanism, two potential surfaces remain parallel until the system reaches the region of strong interaction. When this region is reached, the interaction suddenly gets strong and the mixing of two surfaces takes place. This region is considered to lie around the boundary between the separated

and united atom-molecule regions and is expected to be at fairly large intermolecular distances. Since the probability of a nonadiabatic transition via this mechanism depends on the collision energy,[17] it may be reasonable that the nonadiabatic transition at large intermolecular distances is not effective at low collision energies. Experimentally the threshold for $Ar^+ + HCl \rightarrow Ar + HCl^+(A^2\Sigma)$ is estimated to be 0.79 eV,[6] which is somewhat larger than the endothermicity of the reaction, 0.47 eV. Hence it is reasonable that at the lowest collision energy, 0.71 eV, the transition can not take place between the two surfaces at large reactants' separation.

At low collision energies, a complex mechanism has been proposed for this reaction system.[6,8] The collision energy dependence observed in the SIFDT experiment was explained by a switching of the reaction mechanism from a complex mechanism to a direct one and the former was proposed to be dominant below 0.5 eV of the collision energy.[6] Our coincidence TOF spectra for the HA channel are inconsistent with this long-lived complex mechanism but could be consistent with the SIFDT results because our collision energies are higher than 0.5 eV. Since the nonadiabatic transition at large separation is not attainable at low collision energies, the reactions must be occurring only at short intermolecular distances. In the C_s symmetry, A′ and A″ surfaces evolve from $Ar^+(^2P_j) + HCl\ (X^1\Sigma)$, whereas only A′ surface evolves from $Ar(^1S) + HCl^+(A^2\Sigma)$. At short distances, the interaction between these two A′ surfaces may open a pathway that leads the reactant adiabatically to the charge transfer product $HCl^+(A)$. Thus two product channels, as well as the reaction back to the reactants, are possible from this part of the potential surface. Firstly, ArH^+ is formed by proton-transfer following the electron transfer. Secondly, the system can dissociate into both $HCl^+(A^2\Sigma)$ and $HCl^+(X^2\Pi)$, the dissociation into the latter being highly exothermic and hence likely to be dominant.

At higher collision energies, the agreement between the calculated and observed ratios becomes better for the CT channel (Fig. 4(a)). This is reasonable because the nonadiabatic transition from the $Ar^+ + HCl$ surface to the $Ar + HCl^+(A^2\Sigma)$ one at large separation is now energetically accessible. The formation of $HCl^+(A^2\Sigma)$ is more likely and $HCl^+(X^2\Pi)$ is expected to be formed from the former by radiative transition and/or internal conversion. The formation of $HCl^+(A^2\Sigma)$ by a direct mechanism at high collision energies has been suggested in the SIFDT study as the origin of the increase in the rate constant.[6]

The proton transfer following electron jump leads to the HA product, ArH^+. This sequential mechanism is consistent with the observed peak position of ArH^+ in the coincidence TOF spectra. One result that we still have to explain is the ratios of the cross sections for the HA channel, i.e. the fact that the observed ratios $\sigma(1/2)/\sigma(3/2)$ are much smaller than the calculated ones, as shown in Fig. 4(b). Considering the proposed mechanism in which HA is regarded as CT followed by the proton-transfer, this discrepancy is attributed to the latter half of the mechanism. A similar trend has previously been observed in the reaction $Ar^+ + H_2$,[1] i.e., the cross sections for the HA channel of $Ar^+(^2P_{1/2})$ are only 50% larger than those of $Ar^+(^2P_{3/2})$, whereas the cross sections for the CT channel of $Ar^+(^2P_{1/2})$ are almost ten times larger than those of $Ar^+(^2P_{3/2})$. These results were explained by the model in which the HA channel requires more intimate encounters. Practically, the critical impact parameter b_c based on the Langevin-type calculation was introduced for the collisions leading to ArH^+. This restriction obscured the effect of the spin-orbit excitation on the reaction cross sections very much. The same situation may be applicable to the present $Ar^+ + HCl$ system, and the effect of the spin-orbit states is less pronounced in the HA channel than in the CT channel.

The formation of $HCl^+(A^2\Sigma)$ has also been observed in the ion-beam chemiluminescence experiment.[8] However, the authors of this study insist that $HCl^+(A^2\Sigma)$ is formed by the complex mechanism at collision energies lower than 10 eV based on the fact that the cross section decreases with increasing collision energy. They also recognized a significant discrepancy between the observed vibrational distribution and the Franck–Condon factor distribution. However, our results suggest that the complex formation is unlikely for both the HA and CT channels; the coincidence TOF spectrum of ArH^+ is not consistent with the complex mechanism. The ratios of the CT cross sections for the two spin-orbit states are reasonably well represented by the model based on the direct mechanism. One possible explanation for the discrepancy between the Franck–Condon factors and the observed vibrational distribution is the branching ratio for the two channels as a function of the vibrational level of $HCl^+(A^2\Sigma)$, i.e., higher vibrational levels may be more favorable for the proton transfer to form ArH^+. The decrease in the cross section for $HCl^+(A^2\Sigma)$ may also be explained by the increase of the ArH^+ formation with the increase of the collision energy. In our results, the cross sections for the CT channel slightly decrease compared with those for the HA channel from $E_{coll} = 2.5$ to 3.5. However, an increase in the collision energy also causes the change of collection efficiencies for the secondary ions, better for ArH^+ and worse for HCl^+, then the decrease of the cross sections for CT is not conclusive.

Summary

The reaction $Ar^+(^2P_j) + HCl$ was studied by using the threshold electron-secondary ion coincidence technique. The relative reaction cross sections for the two spin-orbit states, $j = 3/2$ and 1/2, were determined for each of the two product channels, the hydrogen atom abstraction and charge-transfer reactions, at several collision energies. The results were compared with those of a simple model calculation based on the molecular properties at infinite separation, i.e., the energy defects and the Franck–Condon factors. For the CT channel, the agreement was reasonably good at high collision energies but was poor at low collision energies. The observed ratios for the HA channel were always near unity and much smaller than the calculated ones. These results suggest that the nonadiabatic transitions from the $Ar^+(^2P_j) + HCl$ surface to the $Ar + HCl^+(A^2\Sigma)$ surface (charge transfer) at large intermolecular separation are important at high collision energies and that ArH^+ is formed by the proton transfer following this transition. At low collision energies, this mechanism is not dominant because of the energy barrier and more intimate collision plays an important role. However, the formation of a long-lived complex is not suggested because the coincidence TOF spectra showed that ArH^+ has much higher velocity than that

expected for a complex mechanism.

References

1 K. Tanaka, J. Durup, T. Kato, and I. Koyano, *J. Chem. Phys.*, **74**, 5561 (1981).

2 T. Kato, *J. Chem. Phys.*, **80**, 6105 (1984).

3 Electronically excited state of Ar^+ is high lying and does not contribute to reaction studied in near thermal energy.

4 T. Kato, K. Tanaka, and I. Koyano, *J. Chem. Phys.*, **77**, 337 (1982); T. Kato, K. Tanaka, and I. Koyano, *J. Chem. Phys.*, **79**, 5969 (1983); T. Kato, K. Tanaka, and I. Koyano, *J. Chem. Phys.*, **77**, 834 (1982).

5 S. G. Lias, *Int. J. Mass Spectro. Ion Phys.*, **20**, 123 (1976).

6 J. Golsik, W. Freysinger, A. Hansel, P. Spanel, and W. Lindinger, *J. Chem. Phys.*, **98**, 6995 (1995).

7 A. A. Viggiano, R. A. Morris, F. Dale, J. F. Paulson, K. Giles, D. Smith, and T. Su, *J. Chem. Phys.*, **93**, 1149 (1990).

8 Th. Glenewinkel-Meyer and Ch. Ottinger, *J. Chem. Phys.*, **100**, 1148 (1994).

9 P. J. Kuntz and A. C. Roach, *J. Chem. Soc., Faraday Trans. 2*, **68**, 259 (1972).

10 K. Tanaka and I. Koyano, *J. Chem. Phys.*, **69**, 3422 (1978); I. Koyano and K. Tanaka, *J. Chem. Phys.*, **72**, 4858 (1980).

11 S. Suzuki, *J. Chem. Phys.*, **93**, 4102 (1990).

12 D. Rapp and W. E. Francis, *J. Chem. Phys.*, **37**, 2631 (1962).

13 T. Ibuki, N. Sato, and S. Iwata, *J. Chem. Phys.*, **79**, 4805 (1983).

14 H. Hotop, G. Hubler, and L. Kaufhold, *Int. J. Mass Spectrom. Ion Phys.*, **17**, 163 (1975).

15 K. Kimura, S. Katumata, Y. Achiba, T. Yamasaki, and S. Iwata, "Handbook of HeI photoelectron spectra of fundamental organic molecules," Japan Scientific Society (1981).

16 The reaction system, $Ar^+ + CO$ (Ref. 4), where the nonadiabatic transition at large intermolecular separation does not operate shows severe disagreement between the observed and calculated ratios.

17 M. S. Child, "Electronic Excitation: Nonadiabatic Transitions" in "Atom-Molecule Collision Theory," ed by R. B. Bernstein, Plenum Press, New York (1979).